



HAL
open science

Towards Automatic Acne Detection Using a MRF Model with Chromophore Descriptors

Zhao Liu, Josiane Zerubia

► **To cite this version:**

Zhao Liu, Josiane Zerubia. Towards Automatic Acne Detection Using a MRF Model with Chromophore Descriptors. European Signal Processing Conference (EUSIPCO), Sep 2013, Marrakech, Morocco. hal-00863046

HAL Id: hal-00863046

<https://inria.hal.science/hal-00863046>

Submitted on 18 Sep 2013

HAL is a multi-disciplinary open access archive for the deposit and dissemination of scientific research documents, whether they are published or not. The documents may come from teaching and research institutions in France or abroad, or from public or private research centers.

L'archive ouverte pluridisciplinaire **HAL**, est destinée au dépôt et à la diffusion de documents scientifiques de niveau recherche, publiés ou non, émanant des établissements d'enseignement et de recherche français ou étrangers, des laboratoires publics ou privés.

Towards Automatic Acne Detection Using a MRF Model with Chromophore Descriptors

Zhao Liu, Josiane Zerubia

Ayin Research Group, INRIA Sophia Antipolis Méditerranée, France

ABSTRACT

This paper proposes a new acne detection approach using a Markov random field (MRF) model and chromophore descriptors extracted by bilateral decomposition. Compared to most existing acne segmentation methods, the proposed algorithm enables to cope with large-dynamic-range intensity usually existing in conventional RGB acne images captured under uncontrolled environment. Algorithm performance has been tested on acne images of human face from a free public database. Experimental results show that acne segmentation derived from this new approach highly agrees to human visual inspection. Moreover, inflammatory response and hyperpigmentation scar can be well discriminated. It is expected that a computer-assisted diagnostic system for acne severity evaluation will be constructed as a consequence of the present work.

Index Terms— image segmentation, acne detection, chromophore descriptors, Markov random fields (MRFs).

1. INTRODUCTION

Acne vulgaris, a highly prevalent skin disease, has a significant life quality impact on sufferers. It is generally believed that this type of skin disorder results from proliferation of propionibacterium acnes in pilosebaceous units [1]. It can lead to inflammatory lesions (papules, pustules, nodules and cysts) due to increase of oxyhemoglobin level. Dark scarring, known as post-inflammatory hyperpigmentation, will appear thereafter thanks to the excess melanin production [1].

So far there is no golden standard for acne diagnosis in clinics. It entirely depends on dermatologists' experience for acne severity evaluation [2]. But significant variability among individual assessment may lead to less trustworthy diagnosis when several clinicians get involved in the study. In addition, less reproducibility of human evaluation makes comparison of acne changes over time difficult.

With the development of imaging techniques and wide availability of digital cameras, an automatic acne detection and evaluation system should be constructed for assisting dermatologists to achieve more reliable assessment. Such a

computer-based tool would also benefit the development of better skin care products, if it can effectively characterize product's treatment effects in individual skin layers in agreement with physiological understanding.

2. RELATED WORKS

Acne segmentation is normally considered as the first significant step towards an automatic acne grading system, and greatly influences the goodness of acne severity evaluation. A number of studies have been investigated to achieve automatic acne detection. According to the type of experimental data used, they can be mainly classified as methods based on non-RGB photographs and methods using conventional RGB images.

Lucchina et al. [3] utilized a fluorescence spectroscopy imaging technique to evaluate mild to moderate acne after treatment. Fujii et al. [4] isolated inflammatory acne lesions and secondary scars from surrounding healthy skin using Fisher linear discriminant analysis in 16-band multispectral images. These methods show effectiveness on characterizing acne pigmentation levels for automatic lesion detection. But fluorescence images and multispectral data are not always available in clinics and research laboratories. This limits the practicability of these approaches.

On the other hand, Min et al. [2] detected non-inflammatory and inflammatory acne lesions in RGB skin images captured by a well calibrated data acquisition system. Ramli et al. [5] segmented acne lesions using kmeans clustering with CIE Lab color features. Dey et al. [6] minimized the Mahalanobis distance to separate distributions between acne scar and normal skin in RGB and HSI color spaces. The methods stated above perform a content-based segmentation using color descriptors in RGB model or its transformations. However skin color, represented in a specific color space, is not a genuine physical quantity, but a concept based on human visual perception [7]. It sometimes fails to provide precise information about the concentrations of cutaneous chromophores, and is easily influenced by imaging complexities. This may explain the reason why Min's method required skin data captured under ideal experimental environment, and Ramli's approach and Dey's algorithm only tested on small skin areas of acne images.

This paper proposes a new acne detection approach using a Markov random field (MRF) model [8] associating chromophore descriptors. Compared to most existing acne segmentation approaches, the proposed method enables to cope with highlight and strong shading usually existing in RGB skin images captured under uncontrolled environment. Segmentation results of acne images from a free public database [9] show the effectiveness of this new approach for automatic acne detection, which is of great importance to construct a computer-assisted diagnostic system for acne severity evaluation.

3. CHROMOPHORE DESCRIPTORS

In this section, optical theory of human skin is first briefly explained to facilitate the identification of pigments and structures that give rise to skin colors. A new chromophore extraction method based on bilateral decomposition is then described.

3.1. Spectral Reflectance of Human Skin

Optical response of human skin is complex to model accurately because it is not merely a planar reflectance. Absorption, reflection and scattering effects of various components beneath the skin surface have to be considered as a whole. According to [10], human skin can be simplified as a thin structure with distinctive multiple layers, which correspond to epidermis, dermis, and subcutis with collagen and fat. Two major chromophores, melanin and hemoglobin, strongly absorb incident light onto skin surface in epidermis and dermis layers respectively; while spectral absorption of other minor chromophores (e.g. β -carotene) was reported almost negligible as opposed to those of major ones [10]. The dermal collagen thereafter diffusely reflects a large proportion of remaining light, regardless of the wavelength. As such, the pigmentation appearance of human skin is primarily attributed to the absorbance of melanin and hemoglobin, as well as the diffuse reflectance at the collagen/fat layer. As such, spectral reflectance of human skin illuminated by light of wavelength λ at pixel x is [10]:

$$R_{skin}(x, \lambda) = e^{-2(u_m^\lambda l_m^\lambda c_{x,m} + u_h^\lambda l_h^\lambda c_{x,h})} R_{diff}$$

where u_m^λ and u_h^λ are wavelength-dependent absorptive coefficients of melanin and hemoglobin in epidermis and dermis, respectively. $c_{x,m}$ and $c_{x,h}$ donate the concentrations of these two chromophores in a sampled volume of human skin. l_m^λ and l_h^λ represent the lengths of light path in epidermis and dermis layers. R_{diff} is the reflectance coefficient, whose value is $R_{diff} \approx 1$ provided that subcutis is a perfectly diffuse reflected layer [10].

3.2 Chromophore Extraction

Associating skin spectral reflectance with color image formation, image intensity at wavelength λ is given by [11]:

$$I_{x,\lambda} = w_x \int e^{-2(u_m^\lambda l_m^\lambda c_{x,m} + u_h^\lambda l_h^\lambda c_{x,h})} U_{x,\lambda} Q_\lambda d\lambda$$

where Q_λ stands for sensor characteristics, and w_x donates wavelength-independent Lambertian shading, which is the dot product ($w_x = N_x V$) between surface normal (N_x) and lighting direction (V). Taking the Wien's approximation [12] for illumination spectral power distribution $U_{x,\lambda} \cong S_x k_1 \lambda^{-5} e^{-k_2/(\lambda T)}$ (S_x is the lighting intensity, T is the temperature of the black body, k_1 and k_2 are constants), image intensity can be formulated by a linear combination of chromophore coefficients, optical parameters of light source, and effects of scene geometry in an inverse logarithmic form:

$$I_{x,\lambda} = (u_m^\lambda l_m^\lambda c_{x,m} + u_h^\lambda l_h^\lambda c_{x,h}) + \frac{k_2}{\lambda T} - \log S_x - \log \frac{k_1}{\lambda^5} - \log Q_\lambda - \log V - \log N_x$$

Bilateral filter, initially proposed in [13], was developed for image denoising meanwhile preserving important edges and features. It extends the concept of Gaussian smoothing through a weighted average process of neighboring pixels. Applying the bilateral filter on the inverse logarithmic grayscale skin image, the output intensity $I'_{x,\lambda}$ at pixel x is:

$$I'_{x,\lambda} = \frac{1}{A} \sum_{p \in \Omega_x} f(p, x) g(I_{p,\lambda}, I_{x,\lambda}) I_{p,\lambda} \\ = \left[\frac{k_2}{\lambda T} - \log \frac{k_1}{\lambda^5} - \log Q_\lambda - \log V \right] + \\ \left[\frac{1}{A} \sum_{p \in \Omega_x} f(p, x) g(I_{p,\lambda}, I_{x,\lambda}) (u_m^\lambda l_m^\lambda c_{p,m} + u_h^\lambda l_h^\lambda c_{p,h} - \log S_p - \log N_p) \right]$$

where p belongs to the neighborhood (Ω_x) of pixel x , and A is a normalizing constant. The first term of the above equation corresponds to illumination information (a function of λ). The second term contains chromophore reflectance ($u^\lambda l^\lambda c_x$) and shading effects (S_x, N_x), whose contributions in $I'_{x,\lambda}$ are controlled by the spatial function f and the range function g , defined as Gaussian kernels in this study.

Considering that shading is a low frequency component which changes gradually across large skin areas, high frequency chromophore elements can be smoothed out by selecting a relatively large intensity variation. Intrinsic chromophore information can be derived by subtracting $I'_{x,\lambda}$ from $I_{x,\lambda}$. We then embed this bilateral filtering in an iterative process such that chromophore reflectance will iteratively propagate until the difference between images before and after filtering is smaller than a threshold t for every pixel. In this study, $t = 0.01 * \ln(255) \approx 0.05$, which corresponds to 1% of the overall image intensity range.

Therefore, a skin image can be decomposed into a base layer having low frequency imaging factors, and a detail layer containing chromophore reflectance with a small part of high frequency wavelength-independent artifacts (ϵ_x).

$$I_{x,\lambda}^{base} = \frac{k_2}{\lambda T} - \log \frac{k_1}{\lambda^5} - \log Q_\lambda - \log V - \log S_x - \log N_x \\ I_{x,\lambda}^{detail} = u_m^\lambda l_m^\lambda c_{x,m} + u_h^\lambda l_h^\lambda c_{x,h} + \epsilon_x$$

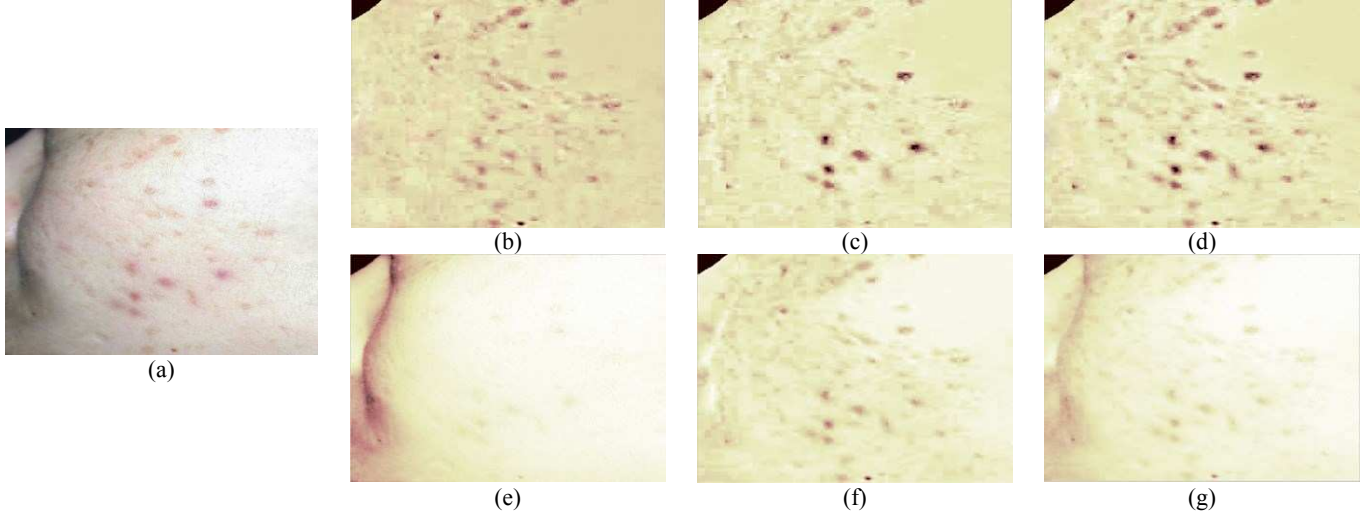


Fig. 1 MI, HI and CI mappings of a conventional RGB acne image from a free public database [9], with highlight and shading as artifacts. (a) original image. (b) MI (c) HI (d) CI mappings, calculated by the bilateral decomposition. (e) the first component, (f) the second component by the ICA method, and (g) the summation of them.

Considering the increased spectrum attenuation of hemoglobin at longer wavelength ($>620\text{nm}$) [14], image intensity in red channel ($\sim 650\text{nm}$) is primarily attributed to melanin concentration, while those of green ($\sim 545\text{nm}$) and blue ($\sim 475\text{nm}$) channels are the joint effects of melanin and hemoglobin, simultaneously. Provided that absorptive coefficients and light penetration lengths can be determined according to the previous publications [15, 16], melanin density and hemoglobin density can be estimated as:

$$\begin{pmatrix} c_{x,m} \\ c_{x,h} \end{pmatrix} = \begin{pmatrix} u_m^g l_m^g - u_m^r l_m^r & u_h^g l_h^g \\ u_m^b l_m^b - u_m^r l_m^r & u_h^b l_h^b \\ u_m^b l_m^b - u_m^g l_m^g & u_h^b l_h^b - u_h^g l_h^g \end{pmatrix}^{-1} \begin{pmatrix} I_{x,g}^{\text{detail}} - I_{x,r}^{\text{detail}} \\ I_{x,b}^{\text{detail}} - I_{x,r}^{\text{detail}} \\ I_{x,b}^{\text{detail}} - I_{x,g}^{\text{detail}} \end{pmatrix} \\ = \begin{pmatrix} 0.176 & 0.747 & 1.042 \\ 0.086 & 0.352 & -0.488 \end{pmatrix} \begin{pmatrix} I_{x,g}^{\text{detail}} - I_{x,r}^{\text{detail}} \\ I_{x,b}^{\text{detail}} - I_{x,r}^{\text{detail}} \\ I_{x,b}^{\text{detail}} - I_{x,g}^{\text{detail}} \end{pmatrix}$$

In this study, the melanin index (MI) and the hemoglobin index (HI) are defined as the normalized c_m and normalized c_h , respectively. In addition, a combined chromophore index $CI = MI + HI$ is generated to represent the joint pigmentation status.

Fig. 1 shows the MI , HI and CI mappings of a conventional RGB acne image calculated by the bilateral decomposition and a widely applied independent component analysis (ICA) approach [11]. Compared to the ICA method, chromophore descriptors from the proposed method are more robust to highlight and shading effects. Moreover, MI and HI mappings are well identified in our method. But this discrimination will not be available in the ICA approach, since it does not incorporate the knowledge of absorbance spectrum of major chromophores, and is only responsible for separating the skin image into two independent components.

4. ACNE DETECTION USING A MRF MODEL

Markov random fields (MRFs) enable to specify the global characteristics of an image in a local manner, and are powerful for modeling spatial interactions in an image [8]. In the present study, a MRF model is used for automatic acne detection.

4.1 Definition of Energy Function

Suppose $D = \{d_x\}_{x \in S}$, where d_x stands for gray-level intensity at pixel x . $L = \{l_i\}, \forall l_i \in [1, R]$ is a set of labels corresponding to R classes. The objective for image classification and acne detection is to find a labeling $F = \{f_x\}_{x \in S}$ taking value from the label set L , which maximizes probability $P(f|D)$ based on the maximum a posteriori (MAP) criterion. According to Hammersley-Clifford theorem, a MRF is equivalent to a Gibbs random field, so the optimization problem turns out to minimize the following energy function [8], with the assumptions that $P(D|f) = \prod_{x \in S} P(d_x|f_x)$ and that $P(d_x|f_x)$ is Gaussian:

$$E_{f_x \in F} = \sum_{x \in S} \left(\frac{\|d_x - \mu_{f_x}\|^2}{2\sigma_{f_x}^2} + \log(\sqrt{2\pi}\sigma_{f_x}) \right) + \sum_{x \in S} \sum_{p \in C_x} \beta \delta(f_x, f_p) \\ \delta(f_x, f_p) = \begin{cases} 1 & f_x \neq f_p \\ 0 & f_x = f_p \end{cases} \quad (\beta > 0)$$

where μ_{f_x} and σ_{f_x} are the mean value and standard deviation of class l_i , provided that f_x taking value l_i from L . C_x is a set of cliques containing $x \in S$ with regard to the chosen neighborhood. β is the Potts parameter controlling the homogeneity of each class. The first part of this equation is called the data term and is related to the likelihood, while the second part represents the penalty of assigning different labels to neighboring pixels and is related to the prior.

4.2 Iterative Segmentation

In the present study, acne segmentation is achieved through minimizing the energy function described in Section 4.1 using the ICM (iterated conditional modes [17]), which gives fast results but requires good initial conditions. Therefore, we propose to embed ICM within an iterative algorithm, improving the initial conditions at each step:

Input: Skin image chromophore intensity D , number of classes R , and a random label field F .

Output: Acne segmentation mask M .

Initialization ($k=0$): D is firstly grouped into R classes by kmeans clustering, compute mean (μ_{l_i}) and standard deviation (σ_{l_i}) of each class l_i and take these value as initial conditions. We initialize the Potts parameter as $\beta = 1$ and compute the Gibbs energy $E_{f_x \in F}$ of label field $f_x \in F$.

Iteration:

(1) Based on initialization ($k = 0$) or the last iteration outputs ($k > 0$), compute energy $E_{f_x \in F}$ of F .

(2) Optimize $E_{f_x \in F}$ using the ICM criterion till the energy change (ΔE) fulfills $\frac{\Delta E}{E} < 0.001$. Record the new label field F' and its Gibbs energy $E'_{f_x \in F'}$.

(3) Compute μ'_{l_i} and σ'_{l_i} of R classes with regard to the new label field F' .

(4) If $\frac{\mu'_{l_i} - \mu_{l_i}}{\mu_{l_i}} \geq 0.01$, update related parameters as $\mu_{l_i} = \mu'_{l_i}$, $\sigma_{l_i} = \sigma'_{l_i}$, $\forall l_i \in [1, R]$; and $F = F'$, $E_{f_x \in F} = E'_{f_x \in F'}$. Then repeat steps (1)-(4) with $k=k+1$.

Otherwise, step out of the iteration. The final acne segmentation mask is $M = F'$.

Here the ICM is chosen due to its computation efficiency. For a skin image (480*640 pixels) in Fig.1(a), it only takes 48.30 seconds for segmentation under Matlab on a computer of Intel(R) Core E5-2630 CPU @2.30 GHz. The number of classes R is defined as the value that maximizes the ratio between inter-cluster minimum distance and mean intra-cluster distance. In the case of Fig.1(a), $R=3$.

4.3. Post-processing

Since acne results from hair follicle blockage by oil and dead skin cells, its shape (especially for mild to moderate acne) usually resembles to that of hair follicle, as circle or ellipse. Hence, shape analysis of detected suspicious acne areas is performed as the post-processing in this study.

Specifically, we (1) find geometry center of each segmented areas, and calculate distance ρ from geometry center to border points in a polar coordinate; (2) normalize the distance ρ by its mean value $\bar{\rho}$ of the detected area, so that $\rho/\bar{\rho}$ is scale-invariant; (3) plot normalized distance $\rho/\bar{\rho}$ in 1D space from 0 to 2π .

Fig.2 shows acne-like shapes versus a non-acne-like shape, with the corresponding normalized distance $\rho/\bar{\rho}$. Both typical and atypical acne-like shapes give positive distance values in the polar coordinate. Whereas the non-

acne-like shape, similar to the areas around nose and mouth, has a large proportion of zero values, since its geometry center lies outside the overall shape area. Hence the non-acne-like areas can be eliminated by setting a threshold with regard to $\rho/\bar{\rho}$, whose value is set as 0 in this work.

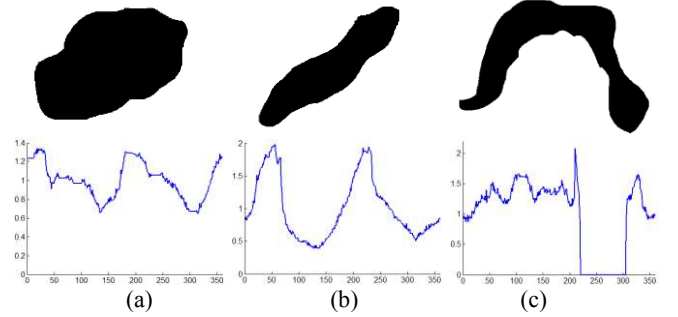


Fig. 2 Shapes of acne-like areas and a non-acne-like area. (a) typical acne-like shape. (b) atypical acne-like shape. (c) non-acne-like shape resembles to areas around nose and mouth, which may exhibit ambiguous pigmentation values with regard to acne.

4.4. Discrimination of Inflammatory Response and Secondary Hyperpigmentation

Finally, the resulting segmentation mask is projected back onto the normalized melanin mapping and hemoglobin mapping, respectively. Calculating the average MI and HI values of normal skin (μ_{skin}), the relative melanin mapping and hemoglobin mapping can then be defined as:

$$MI_{rel} = MI - \mu_{skin}(MI)$$

$$HI_{rel} = HI - \mu_{skin}(HI)$$

For a segmented acne area (α), if its average value in relative HI mapping is larger than the average value in relative MI mapping, the acne is supposed as inflammatory; otherwise it is considered as post-inflammatory hyperpigmentation.

$$\begin{cases} HI_{rel,\alpha} \geq MI_{rel,\alpha} & \alpha \text{ is inflammatory acne} \\ HI_{rel,\alpha} < MI_{rel,\alpha} & \alpha \text{ is hyperpigmentation} \end{cases}$$

4. EXPERIMENTAL RESULTS

In the experiment, the combined pigmentation mapping CI is used as the only segmentation feature and forwarded to the iterative algorithm described in Section 4.2, to isolate acne from surrounding normal skin. 50 challenging RGB acne images [9], captured under uncontrolled environment, has been tested in this study. Fig. 3 shows five randomly selected examples and their corresponding segmentation results, with discrimination between inflammatory responses and hyperpigmentation scars. The automatic acne detection is highly consistent to human visual inspection, regardless of various external imaging factors.



Fig. 3 Acne segmentation of five acne images from a public database [9]. First row: original images with highlight or shading/shadows due to scene geometry. Second row: segmentation results using the MRF model and chromophore descriptors. Inflammatory acne is outlined by the blue line, and hyperpigmentation is outlined by the black line.

Professional evaluation of the derived segmentation results is currently under process by an experienced dermatologist from a hospital (CHU Nice). Based on expert assessment, segmentation accuracy by the proposed method will be quantitatively evaluated in the future.

5. CONCLUSIONS

This paper proposes an automatic acne detection method through incorporating a MRF model and chromophore descriptors extracted by bilateral decomposition. Experimental results show that the proposed algorithm is robust to large-dynamic-range intensity, hence enables to work on skin color images captured under uncontrolled environment. The derived automatic acne segmentation results appear to be highly consistent to human visual assessment. It is expected that a computer-assisted diagnostic system for acne severity evaluation will be constructed in the future using the proposed method.

6. ACKNOWLEDGMENT

The first author would like to thank INRIA-DPE for the funding of Postdoctoral Fellowship. This research study has been conducted within the LIRA Consortium.

7. REFERENCES

- [1] G.F. Webster. "Inflammation of acne vulgaris," *Journal of American Academy of Dermatology*, vol.33, pp.247–253, 1995.
- [2] S. Min, H.J. Kong, C. Yoon, H.C. Kim, and D.H. Suh. "Development and evaluation of an automatic acne lesion detection program using digital image processing," *Skin Research and Technology*, vol.0, pp. 1–10, 2012.
- [3] L.C. Lucchina, N. Kollias, R.Gillies, S.B. Phillips, J.A. Muccini, M.J. Stiller, R.J. Trancik, and L.A. Drake. "Fluorescence photography in the evaluation of acne," *Journal of American Academy of Dermatology*, vol.35, pp. 58-63, 1996.
- [4] H. Fujii, T. Yanagisawa, M. Mitsui, Y. Murakami and M. Yamaguchi. "Extraction of acne lesion in acne patients from multispectral images". *In proc. of 30th international conference on*

- Engineering in Medicine and Biology Society (EMBS)*, pp. 4078-4087, Vancouver, 2008.
- [5] R. Ramli, A.S. Malik, A. Hani, and F.B. Yap. "Segmentation of acne vulgaris lesions," *In proc. of Digital Image Computing: Techniques and Applications*, pp. 335-339, Queensland, 2011.
- [6] B.C. Dey, B. Nirmal, and R.R. Galigekere. "Automatic detection of acne scars: Preliminary results," *In proc. of Point-of-Care Healthcare Technologies*, pp. 224-227, Bangalore, 2013.
- [7] B.A. Wandell. *Foundations of vision*, Sinauer Associates, Sunderland, 1995.
- [8] Z. Kato and J. Zerubia. *Markov random fields in image segmentation*, Foundations and Trends in Signal Processing, vol. 5, no 1-2, pp.1-155, 2012.
- [9] Dermnet NZ, the dermatology resource. New Zealand Dermatological Society.
- [10] J. B. Dawson, D.J. Barker, D.J. Ellis, E. Grassam, J.A. Cotterill, G.W. Fisher, and J.W. Feather. "A theoretical and experimental study of light absorption and scattering by in vivo skin," *Physics in Medicine and Biology*, vol. 25, pp. 695–709, 1980.
- [11] N. Tsumura, H. Haneishi, and Y. Miyake. "Independent component analysis of spectral absorbance image in human skin," *Optical Review*, vol.7, pp.479–482, 2000.
- [12] J. Mehra and H. Rechenberg. *The historical development of quantum theory*, Springer-Verlag, New York, 1982.
- [13] C. Tomasi and R. Manduchi. "Bilateral filtering for gray and color images," *In proc. of 6th International Conference on Computer Vision (ICCV)*, pp. 830-846, New Delhi, 1998.
- [14] T. Igarashi, K. Nishino, and S. Nayar. "The appearance of human skin: a survey," *Foundations and Trends in Computer Graphics and Vision*, vol.3, pp. 1-95, 2007.
- [15] S. Jacques. "Skin optics," *Oregon Medical Laser Center News*, Jan, 1998.
- [16] G.S. Keller, V.G. Lacombe, P. Lee, and J.P. Watson. *Lasers in aesthetic surgery*, Thieme, 2001.
- [17] J. Besag, "On the statistical analysis of dirty pictures," *Journal of the Royal Statistical Society, Series B*, vol. 48, no.3, pp. 259-302, 1986.